Guidance of magnetic space tug

Emilien Fabacher [a], Stéphanie Lizy-Destrez [a,*], Daniel Alazard [a], Finn Ankersen [b], Alexandre Profizi [c]

[a] ISAE-SUPAERO, 10 av. Edouard Belin, 31000 Toulouse, France
[b] European Space Agency, Keplerlaan 1, 2201 AZ Noordwijk, The Netherlands
[c] Airbus-Safran Launchers, 61 route de Verneuil, 78130 Les Mureaux, France

Abstract

Magnetic tugging of a target satellite without thrust capacity can be interesting in various contexts, as for example End-Of-Life management, or to complete launchers capabilities. The aim is to gradually modify the orbit of the target by constantly exerting on it a magnetic force. To do so, the chaser is assumed equipped with a steerable magnetic dipole, able to create both forces and torques on the magnetic torque rods carried by the target. The chaser is also supposed to carry electric thrusters, creating a continuous force which modifies the orbit of the whole formation composed of chaser and target.

The relative motions of both satellites are derived, in order to assess the feasibility of such a concept. Relative configuration (attitudes and position) trajectories are derived, which are compliant with the dynamics, and enable the chaser to tug the target.

Considering targets in Low Earth Orbit (LEO), the magnetic field of the Earth is taken into account, modeled by the International Geomagnetic Reference Field (IGRF). The position of the magnetic torque rod of the target may not be located at its center of mass. This lever-arm is taken into account in the dynamics.

As for every Electro-Magnetic Formation Flight concept developed in the literature, satellites involved in magnetic tugging are constantly subjected to torques, created by the Earth magnetic field and by the magnetic fields created by the other satellites in the formation. In this study, the solution chosen to face this problem is to take into account the attitude equilibrium of the satellites early in the guidance phase, in order to avoid having to wave the dipole, as it is generally done.

Promising results are presented for different types of orbit, showing that the concept could be feasible in many different scenarios.

Keywords: Space tug; Electromagnetic formation flying; Active debris removal

For a given vector $\mathbf{x}, x$ is the norm of the vector, and $\hat{\mathbf{x}}$ is the unitary vector associated. Scalar variables are never represented by bold letters. With the exception of **F** (a force) and **B** (a magnetic field), upper-case bold letters refer to non-vector matrices. $[\mathbf{x}]$ is the skew-symmetric matrix denoting the cross-product $\mathbf{x}\times$ and $\dot{\mathbf{x}}$ denotes the time derivation in the orbital frame: $\dot{\mathbf{x}} = \frac{d\mathbf{x}}{dt}|_{\mathcal{O}}$.

Subscripts are used to give precision on the variables. A maximum of four subscripts are used, in the order defined here: the first one defines the object concerned. The second one refers to the cause. The third one is the axis considered, and the fourth defines projection frame. For example, $F_{C_{thx_{\mathcal{O}}}}$ is the projection of the thruster force applied on the chaser along the x-axis of the orbital frame. To lighten equations, this notation is reduced when the clarity is unaf-

* Corresponding author.
E-mail addresses: emilien.fabacher@isae.fr (E. Fabacher), stephanie.lizy-destrez@isae.fr (S. Lizy-Destrez), daniel.alazard@isae.fr (D. Alazard), finn.ankersen@esa.int (F. Ankersen), alexandre.profizi@airbusafran-launchers.com (A. Profizi).

http://dx.doi.org/10.1016/j.asr.2017.03.042
0273-1177

Nomenclature

Constants

μ_0	magnetic constant ($\mu_0 = 4\pi 10^{-7}$ N/A^2)
μ	standard gravitational parameter of the Earth ($\mu = 3.986\ 10^{14}$ m^3/s^2)

Variables

$\mathbf{F}$	force (N)
$\mathbf{f}$	force per unit of mass (N/kg)
$\mathbf{B}$	magnetic field (T)
$\boldsymbol{\tau}$	torque (Nm)
$\boldsymbol{\mu}$	magnetic dipoles, always with subscript (Am^2)
$\mathbf{d}$	vector from chaser dipole to target dipole (m)
$\mathbf{s}$	vector from target center of mass to the chaser center of mass (m)
$\mathbf{s}_i$	vector from formation center of mass to satellite i center of mass (m)
$\boldsymbol{\theta}$	vector of Euler angles describing the attitude of the target in orbital frame
$\mathbf{r}$	vector from Earth center to the point considered (m)
γ_{μ_T}	vector from target center of mass to the target dipole (m)
m	spacecraft mass (kg)
m_{CT}	reduced mass: $m_{CT} = \frac{m_C m_T}{m_C + m_T}$
$\boldsymbol{\omega}$	rotation vector from inertial to orbital frame
$\mathbf{J}$	spacecraft inertia matrix in spacecraft body frame
$\mathbf{I}_l$	identity matrix of size l
$\mathbf{P}_{\mathcal{O}\to\mathcal{T}}$	rotation matrix from frame $\mathcal{O}$ to $\mathcal{T}$: $\mathbf{x}_\mathcal{T} = \mathbf{P}_{\mathcal{O}\to\mathcal{T}}\mathbf{x}_\mathcal{O}$

Subscript

$\mathcal{I}$	inertial frame
$\mathcal{O}$	orbital frame
$\mathcal{C}$	chaser body frame
$\mathcal{T}$	target body frame
C	chaser satellite
T	target satellite
i	either C or T
CoM	center of mass of the formation
g	gravity or gravity gradient
$\epsilon\mu$	electromagnetic
E	due to the Earth
γ	due to the lever-arm $\boldsymbol{\gamma}_{\mu_T}$
th	thrusters
rw	attitude control system (e.g. reaction wheels)
d	created by the reaction wheels to desaturate them
p	perturbation

fected. For example, $\mathbf{F}_{T_{\epsilon\mu}}$ is the electromagnetic force exerted on the target.

Three frames are used in this article; $\mathcal{I}$, an inertial frame centered on the Center of Mass of the formation (CoM); $\mathcal{O}$, the orbital frame centered on the center of mass of the formation; $\mathcal{T}$, the target body frame. These reference frames are represented in Fig. 1. $\hat{\mathbf{z}}_\mathcal{O}$ is toward the Earth. $\hat{\mathbf{y}}_\mathcal{O}$ is perpendicular to the orbit, in opposition to the angular momentum. $\hat{\mathbf{x}}_\mathcal{O} = \hat{\mathbf{y}}_\mathcal{O} \times \hat{\mathbf{z}}_\mathcal{O}$. These definitions are summarized in Fig. 1.

1. Introduction

Satellite tugging can be motivated by various reasons. It can be for de-orbiting or re-orbiting: for example in the case of satellites having finished their mission, but being unable to do the maneuver by themselves. It can be for orbit management, in the case of a constellation composed of several satellites in which only one is equipped with thrusters for example. It can also be considered as a mean to finalize launches, in which case this maneuver would increase launchers capabilities.

Whatever the reasons, several means can be considered to achieve orbit modification of a satellite by tugging it with another satellite. Indeed, one could simply dock a chaser satellite to the target satellite. In the frame of Active Debris Removal (ADR), contactless solutions however could be more interesting. They could indeed provide a way to avoid the need for standardized interfaces and hazardous uncooperative docking phases, as well as reduce the risk of creating new debris. For example, Schaub and Sternovsky (2014) suggested to use electrostatic forces by charging the surfaces of the target and the chaser with ions of the other polarity, in order to create an attracting force between the two. However, charging satellite surfaces is generally problematic, and can even be hazardous, as pointed out by Garrett (1981). This solution seems therefore adapted mainly for dead satellites.

In this study, which has been briefly presentented in Fabacher et al. (2015), and in the same context as Voirin et al. (2012), solutions using magnetic forces to tug the target are detailed. Indeed many satellites, specially in Low Earth Orbit, are equipped with Magnetic Torque Bars (MTQ) which are devices used for attitude control. MTQ create magnetic fields, which could be used by a chaser equipped with a powerful steerable magnetic dipole, in order to create forces and torques on the target.

Electromagnetic Formation Flying (EMFF) is a concept studied since the beginning of the 21st century. It consists in flying satellites in formation, using magnetic forces and torques to control their relative positions and attitudes. Much theoretical work has already been done, giving this concept a solid framework. Schweighart (2005) solved the

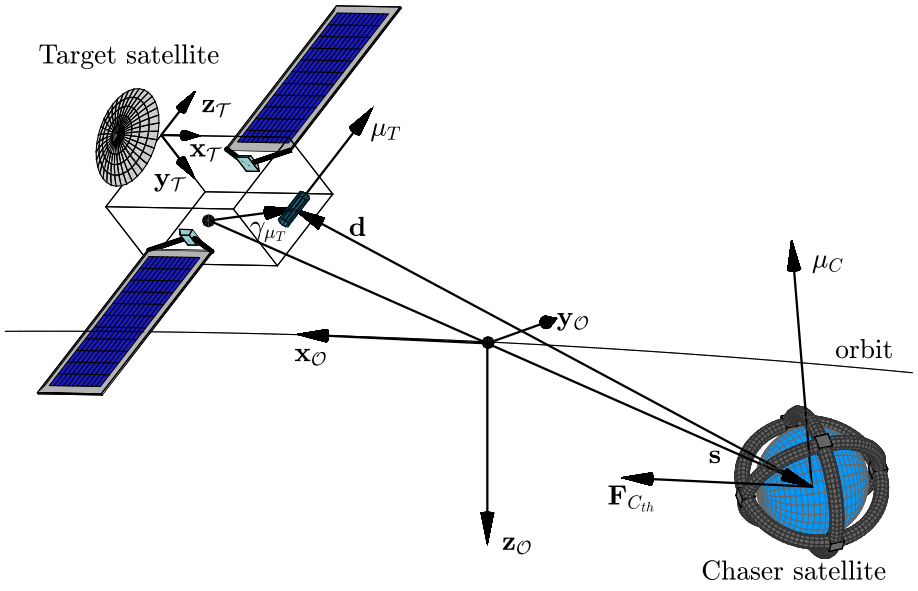

Fig. 1. Representation of the two main frames used in the article: $\mathcal{O}$ and $\mathcal{T}$. The different vectors considered are also represented ($\mathbf{d} = \boldsymbol{\gamma}_{\mu_T} - \mathbf{s}$).

dipole planning problem for a formation composed of N spacecraft, while Ahsun et al. (2007) worked on the control of such a formation. Electromagnetic formations consisting of several cooperative spacecraft have been continuously studied since then: Elias et al. (2007) gave a way to control the relative position of a formation, while controlling the attitudes with reaction wheels on each satellite; Sakai et al. (2008) solved the guidance to keep the same position in time and suggested to wave the dipole to avoid the problem caused by the constant torque due to the Earth magnetic field on each satellite; Ahsun et al. (2010) improved the work done by Elias et al. (2007) and applied an idea similar to Sakai et al. (2008). Recently, Huang et al. (2016) started looking for configurations enabling to reduce the total momentum of a 2-satellites formation.

2. Aim and contribution of this study

The principle of magnetic tugging is quite simple: a chaser/tug satellite, thrusters turned on and equipped with a powerful steerable magnetic dipole creates a magnetic field which attracts the dipole carried by a target/tugged satellite. This problem has already been formulated by Zhang et al. (2014), which gave a first solution. Several facts overlooked by Zhang et al. (2014) however make the realization of this concept complex.

First, the non-trivial orbital dynamics of a pair of spacecraft flying in close proximity is combined to the complex way magnets create forces on one another, and to the existence of constant thrust force created by the chaser satellite. This problem is similar to the ones encountered by Elias et al. (2007), Sakai et al. (2008), Ahsun et al. (2010) and Huang et al. (2016).

Second, the target is not assumed to be able to control its own magnetic dipole. Therefore contrary to Elias et al. (2007), Sakai et al. (2008), Ahsun et al. (2010) and Huang et al. (2016), waving it in order to avoid building up angular momentum because of the Earth magnetic field is not an option.

Third, creating magnetic forces automatically creates torques between the dipoles interacting. Whilst in standard (without propulsion) EMFF, it can be hoped that the torques on all satellites averages to zero, it would not be the case for magnetic tugging, as the maneuver would take a long time, during which the relative configuration could remain the same.

Fourth, the satellites considered by every study up to now are dedicated to EMFF, and particularly, the magnetic dipole they carry is located precisely at its center of mass. Though in our case this can be true for the chaser, the MTQ of the target may be located elsewhere in its structure. This lever-arm adds a torque which has to be taken into account.

Finally, many parameters evolve in orbit around the Earth. The orbital rate and the distance to the Earth for example, if the orbit is not perfectly circular. The most important parameter for magnetic tugging is the Earth magnetic field in orbit, which evolution in orbit is not negligible.

In this paper, focus is made on the orbit transfer of an electromagnetic formation composed of two satellites. The target is considered to be carrying an activated magnetic coil located away from its center of mass, creating a constant magnetic dipole in its body frame. The chaser is supposed fully actuated: not only is it equipped with a steerable magnetic coil, but also with an attitude control system, as well as with an electric propulsion system, able to create thrust in the range 10–100 mN. Chemical propulsion is not considered, because it is not adapted to the small forces that can be created between the magnetic coils.

The core of this study is the dynamics of the formation during the orbit transfer. The issue is the behavior of both satellites, when the formation is subjected to an external force created by the thrusters of the chaser. The aim is to find the configurations (relative position, attitudes, chaser magnetic dipole) which allow the chaser to tug the target. Because of the constantly evolving external magnetic field in orbit, the relative configuration of the formation cannot be constant. Therefore, configurations *paths* will be showed, complying at all time with the dynamics. They enable the chaser to exert a constant acceleration on the target as well as keep the angular momentum of both satellites at low values by counterbalancing the torques which apply. Finally, configurations enabling to desaturated the attitude control system of the satellites will be shown, without impacting the orbit transfer.

To do so, the magnetic framework is developed in Section 3. Section 4 then gives the equations of the relative motions of the two satellites during the orbit transfer, as well as the equation describing the attitude dynamics. Combining Sections 3 and 4 is done in Section 5, which formalizes the whole guidance problem and deals with different possible strategies. The guidance problem is solved in 6 and the results of the study are given in Section 7.

3. Forces and torques between two magnetic coils

The forces and torques created by a magnetic coil on another magnetic coil result from the integration of Biot - Savart law (describing the magnetic field created by an infinitesimal length of conducting wire) and Lorenz force (describing the force exerted by a magnetic field on a infinitesimal length of conducting wire) along the two coils. When the distance between the two coils is greater than roughly eight times the biggest radius of the two coils, the coils can be assimilated to magnetic dipoles. This approximation is valid from far to close rendezvous. In this case, the expressions can be simplified using a first-order Taylor expansion of the complete expressions (Schweighart, 2005; Villani, 1998). Doing so leads to the expressions called "far-field" expressions of the magnetic field, force and torque created by dipole $\boldsymbol{\mu}_1$ on dipole $\boldsymbol{\mu}_2$ when separated by $\mathbf{d}$, vector from 1 to 2:

$$\mathbf{B}_{1/2} = \frac{\mu_0}{4\pi d^3}\left(3\left(\boldsymbol{\mu}_1 \cdot \hat{\mathbf{d}}\right)\hat{\mathbf{d}} - \boldsymbol{\mu}_1\right) \tag{1}$$

$$\mathbf{F}_{1/2} = \frac{3\mu_0}{4\pi d^4}\left((\boldsymbol{\mu}_1 \cdot \boldsymbol{\mu}_2)\hat{\mathbf{d}} + \left(\boldsymbol{\mu}_1 \cdot \hat{\mathbf{d}}\right)\boldsymbol{\mu}_2 + \left(\boldsymbol{\mu}_2 \cdot \hat{\mathbf{d}}\right)\boldsymbol{\mu}_1 - 5\left(\boldsymbol{\mu}_1 \cdot \hat{\mathbf{d}}\right)\left(\boldsymbol{\mu}_2 \cdot \hat{\mathbf{d}}\right)\hat{\mathbf{d}}\right) \tag{2}$$

$$\boldsymbol{\tau}_{1/2} = \boldsymbol{\mu}_2 \times \mathbf{B}_{1/2} = \boldsymbol{\mu}_2 \times \left(\frac{\mu_0}{4\pi d^3}\left(3\left(\boldsymbol{\mu}_1 \cdot \hat{\mathbf{d}}\right)\hat{\mathbf{d}} - \boldsymbol{\mu}_1\right)\right) \tag{3}$$

Expressions (1), (2) and (3) can be written as matrix products in order to simplify their use:

$$\mathbf{B}_{1/2} = \frac{\mu_0}{4\pi}\Gamma(\mathbf{d})\boldsymbol{\mu}_1 \tag{4}$$

$$\mathbf{F}_{1/2} = \frac{3\mu_0}{4\pi}\boldsymbol{\Psi}(\boldsymbol{\mu}_1, \mathbf{d})\boldsymbol{\mu}_2 = \frac{3\mu_0}{4\pi}\boldsymbol{\Psi}(\boldsymbol{\mu}_2, \mathbf{d})\boldsymbol{\mu}_1 \tag{5}$$

$$\boldsymbol{\tau}_{1/2} = \frac{\mu_0}{4\pi}\boldsymbol{\mu}_2 \times \Gamma(\mathbf{d})\boldsymbol{\mu}_1 = \frac{\mu_0}{4\pi}[\boldsymbol{\mu}_2]\Gamma(\mathbf{d})\boldsymbol{\mu}_1 \tag{6}$$

In which one must pay attention to the direction of $\mathbf{d}$. Considering $\mathbf{d}$ from 2 to 1 changes expression (5) to:

$$\mathbf{F}_{1/2} = -\frac{3\mu_0}{4\pi}\boldsymbol{\Psi}(\boldsymbol{\mu}_1, \mathbf{d}_{21})\boldsymbol{\mu}_2 = -\frac{3\mu_0}{4\pi}\boldsymbol{\Psi}(\boldsymbol{\mu}_2, \mathbf{d}_{21})\boldsymbol{\mu}_1 \tag{7}$$

In a given frame, $\boldsymbol{\Psi}$ and Γ are the matrices defined by ($i \in \{1, 2\}$):

$$\boldsymbol{\Psi}_i = \boldsymbol{\Psi}(\boldsymbol{\mu}_i, \mathbf{d}) = -\frac{5}{d^7}(\boldsymbol{\mu}_i \cdot \mathbf{d})\begin{bmatrix} d_x^2 & d_x d_y & d_x d_z \\ d_x d_y & d_y^2 & d_y d_z \\ d_x d_z & d_y d_z & d_z^2 \end{bmatrix} + \frac{(\boldsymbol{\mu}_i \cdot \mathbf{d})}{d^5}\mathbf{I}_3 + \frac{1}{d^5}\begin{bmatrix} 2\mu_{i_x} d_x & \mu_{i_x} d_y + \mu_{i_y} d_x & \mu_{i_x} d_z + \mu_{i_z} d_x \\ \mu_{i_x} d_y + \mu_{i_y} d_x & 2\mu_{i_y} d_y & \mu_{i_y} d_z + \mu_{i_z} d_y \\ \mu_{i_x} d_z + \mu_{i_z} d_x & \mu_{i_y} d_z + \mu_{i_z} d_y & 2\mu_{i_z} d_z \end{bmatrix} \tag{8}$$

$$\Gamma = \Gamma(\mathbf{d}) = \frac{3}{d^5}\begin{bmatrix} d_x^2 & d_x d_y & d_x d_z \\ d_x d_y & d_y^2 & d_y d_z \\ d_x d_z & d_y d_z & d_z^2 \end{bmatrix} - \frac{1}{d^3}\mathbf{I}_3 \tag{9}$$

The determinants of matrices $\boldsymbol{\Psi}_i$ and Γ are:

$$\det(\boldsymbol{\Psi}_i) = -(\boldsymbol{\mu}_i \cdot \mathbf{d})\frac{\left((\boldsymbol{\mu}_i \cdot \mathbf{d})^2 + \boldsymbol{\mu}_i^2 \mathbf{d}^2\right)}{d^{15}} \tag{10}$$

$$\det(\Gamma) = \frac{2}{d^9} \tag{11}$$

Let's consider a steerable dipole $\boldsymbol{\mu}_1$ located at the origin of a frame. The determinant of Γ being always different from zero (for $d > 0$), it is possible to create every desired magnetic field $\mathbf{B}$ at any given point $\mathbf{d}$ in space. To do so, the dipole which must be created at the origin is given by:

$$\boldsymbol{\mu}_1 = \frac{4\pi}{\mu_0}\Gamma^{-1}\mathbf{B} \tag{12}$$

Similarly, if one takes into account another dipole $\boldsymbol{\mu}_2$ located in $\mathbf{d}$, then as long as $(\boldsymbol{\mu}_2 \cdot \mathbf{d}) \neq 0$ it is possible to create any desired force $\mathbf{F}_{1/2}$ on dipole $\boldsymbol{\mu}_2$. Inverting (5) gives the dipole which must be created:

$$\boldsymbol{\mu}_1 = \frac{4\pi}{3\mu_0}\boldsymbol{\Psi}_2^{-1}\mathbf{F}_{1/2} \tag{13}$$

If $(\boldsymbol{\mu}_2 \cdot \mathbf{d}) = 0$ then Eq. (2) becomes:

$$\mathbf{F}_{1/2} = \frac{3\mu_0}{4\pi d^4}\left((\boldsymbol{\mu}_1 \cdot \boldsymbol{\mu}_2)\hat{\mathbf{d}} + \left(\boldsymbol{\mu}_1 \cdot \hat{\mathbf{d}}\right)\boldsymbol{\mu}_2\right) \tag{14}$$

Which shows that in this case, it is not possible to create forces on $\boldsymbol{\mu}_2$ perpendicular to the plane defined by $\boldsymbol{\mu}_2$ and $\mathbf{d}$.

4. EMFF dynamics and guidance equations

In this section, focus is first made on the transfer orbit which would be used by electromagnetic formations. Then, the guidance problem is derived.

4.1. On the transfer orbit

Because the forces which can be created between two magnets are relatively small when considering distances of roughly tens of meters, the thrust that can be applied on the formation to modify its orbit is limited to low values. Indeed, for the formation to be balanced, the thrust must be of the same order of magnitude than the inter-satellite force. Electrical propulsion systems would hence be the best suited to this kind of missions. Therefore, modifying the orbit of the formation would require continuous thrusting during extended period of time. Taking this into account, computing the best thrust profile along the transfer is a complex problem which falls under the techniques of optimal control, for which many references can be found in the literature: see for example Tsien (1953), Coverstone-Carroll et al. (2000) and Pergola (2010). It is not the aim of this study. However because the dynamics of the formation is linked to the thrust exerted by the chaser as it will be seen in Section 4.2, we will suppose given a thrust profile $\mathbf{F}_{C_{th}}(t)$.

To simplify the problem, we will assume that the thrust is constant in time, and aligned with its velocity. This corresponds to the thrust profile modifying the fastest the energy of the orbit, and therefore its semi-major axis. In this case, the orbit followed by the formation would be spiral (Petropoulos, 2002), as represented in Fig. 2. This assumption is not problematic for the work done here, as the resolution method described in Section 6 is adapted to time varying thrust.

4.2. Relative position dynamics

In this section are first derived the equations describing the movement of the formation around its center of mass in the orbital frame. Then, equilibrium conditions are found, enabling the formation to stay in a constant configuration.

The sum of the different forces on satellite i ($i = C$ or T) is:

$$\mathbf{F}_i = \mathbf{F}_{i_g} + \mathbf{F}_{i_{e\mu}} + \mathbf{F}_{i_{th}} + \mathbf{F}_{i_p} \tag{15}$$

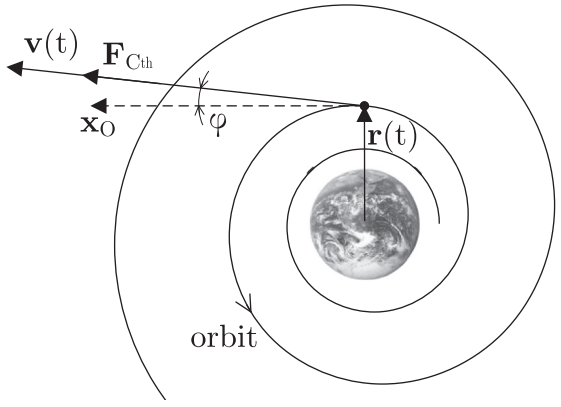

Fig. 2. Transfer orbit. In this case, the aim is to increase the altitude of the orbit.

As:

$$\mathbf{r}_i = \mathbf{r}_{CoM} + \mathbf{s}_i \tag{16}$$

Combining (15) and (16) and applying Newton's second law to each spacecraft yields:

$$\begin{aligned}\frac{d^2\mathbf{s}}{dt^2} &= \frac{d^2\mathbf{s}_C}{dt^2} - \frac{d^2\mathbf{s}_T}{dt^2} \\ &= \frac{d^2\mathbf{r}_C}{dt^2} - \frac{d^2\mathbf{r}_T}{dt^2} \\ &= \mathbf{f}_{C_g} - \mathbf{f}_{T_g} + \frac{\mathbf{F}_{C_{th}}}{m_C} - \frac{\mathbf{F}_{T_{e\mu}}}{m_T} + \frac{\mathbf{F}_{C_{e\mu}}}{m_C} + \Delta\mathbf{f}_p \\ &= \mathbf{f}_{C_g} - \mathbf{f}_{T_g} + \frac{\mathbf{F}_{C_{th}}}{m_C} - \frac{1}{m_C m_T}\left(m_C\mathbf{F}_{T_{e\mu}} - m_T\mathbf{F}_{C_{e\mu}}\right) + \Delta \\ &\mathbf{f}_p\end{aligned} \tag{17}$$

with $\Delta\mathbf{f}_p$ being the difference between the perturbation accelerations on the target and the chaser. Knowing that $\mathbf{F}_{T_{e\mu}} = -\mathbf{F}_{C_{e\mu}}$, Eq. (17) then yields:

$$\frac{d^2\mathbf{s}}{dt^2} = \mathbf{f}_{C_g} - \mathbf{f}_{T_g} + \frac{\mathbf{F}_{C_{th}}}{m_C} - \frac{\mathbf{F}_{T_{e\mu}}}{m_{CT}} + \Delta\mathbf{f}_p \tag{18}$$

With $m_{CT} = \frac{m_C m_T}{m_C + m_T}$. Let's now proceed to a first order approximation of $\mathbf{f}_{i_g}$, knowing that $s_i \ll r_{CoM}$:

$$\begin{aligned}\mathbf{f}_{i_g} &= \mathbf{f}_g(\mathbf{r}_i) \\ &= \mathbf{f}_g(\mathbf{r}_{CoM}) + \frac{\partial \mathbf{f}_g}{\partial \mathbf{r}}|_{\mathbf{r}=\mathbf{r}_{CoM}}(\mathbf{r}_i - \mathbf{r}_{CoM})\end{aligned} \tag{19}$$

Which immediately gives:

$$\begin{aligned}\mathbf{f}_{C_g} - \mathbf{f}_{T_g} &= \frac{\partial \mathbf{f}_g}{\partial \mathbf{r}}|_{\mathbf{r}=\mathbf{r}_{CoM}}(\mathbf{r}_C - \mathbf{r}_T) \\ &= \frac{\partial \mathbf{f}_g}{\partial \mathbf{r}}|_{\mathbf{r}=\mathbf{r}_{CoM}}\mathbf{s} \\ &= -\frac{\mu}{r_{CoM}^3}\mathbf{M}\mathbf{s}\end{aligned} \tag{20}$$

With μ the standard gravitational parameter of the Earth. Let's now note $\mathbf{r}_{CoM} = \begin{bmatrix} r_x & r_y & r_z \end{bmatrix}^T$ in the inertial frame. The Jacobian matrix $\mathbf{M}$ at $\mathbf{r}_{CoM}$ is obtained from Wie (2008):

$$\mathbf{M}_{\mathcal{I}} = \begin{bmatrix} 1 - 3\frac{r_x^2}{r_{CoM}^2} & 3\frac{r_x r_y}{r_{CoM}^2} & 3\frac{r_x r_z}{r_{CoM}^2} \\ 3\frac{r_x r_y}{r_{CoM}^2} & 1 - 3\frac{r_y^2}{r_{CoM}^2} & 3\frac{r_y r_z}{r_{CoM}^2} \\ 3\frac{r_x r_z}{r_{CoM}^2} & 3\frac{r_y r_z}{r_{CoM}^2} & 1 - 3\frac{r_z^2}{r_{CoM}^2} \end{bmatrix} \tag{21}$$

Finally:

$$\frac{d^2\mathbf{s}}{dt^2} = -\frac{\mu}{r_{CoM}^3}\mathbf{M}\mathbf{s} + \frac{\mathbf{F}_{C_{th}}}{m_C} - \frac{\mathbf{F}_{T_{e\mu}}}{m_{CT}} + \Delta\mathbf{f}_p \tag{22}$$

(22) will now be projected in the orbital frame. Differentiating twice in this frame gives Eq. (23).

$$\frac{d^2\mathbf{s}}{dt^2}|_{\mathcal{I}} = \frac{d^2\mathbf{s}}{dt^2}|_{\mathcal{O}} + \boldsymbol{\omega} \times (\boldsymbol{\omega} \times \mathbf{s}) + 2\boldsymbol{\omega} \times \frac{d\mathbf{s}}{dt}|_{\mathcal{O}} + \frac{d\boldsymbol{\omega}}{dt}|_{\mathcal{O}} \times \mathbf{s} \tag{23}$$

Let's now note $\dot{\mathbf{s}} = \frac{d\mathbf{s}}{dt}|_{\mathcal{O}}$ and $\boldsymbol{\eta} = \frac{d\boldsymbol{\omega}}{dt}|_{\mathcal{O}}$. To simplify the notations, $\mathbf{r}_{CoM}$ is simply noted $\mathbf{r}$ from now on. Then the general equation describing the relative motion in orbit is:

$$\ddot{\mathbf{s}} + \boldsymbol{\omega} \times (\boldsymbol{\omega} \times \mathbf{s}) + 2\boldsymbol{\omega} \times \dot{\mathbf{s}} + \boldsymbol{\eta} \times \mathbf{s} + \frac{\mu}{r^3}\mathbf{M}\mathbf{s} = \frac{\mathbf{F}_{C_{th}}}{m_C} - \frac{\mathbf{F}_{T_{\epsilon\mu}}}{m_{CT}} + \Delta\mathbf{f}_p \tag{24}$$

As in the orbital frame $\mathbf{r}_{\mathcal{O}} = [0 \quad 0 \quad -r]^T$, we have $\mathbf{M}_{\mathcal{O}} = \begin{bmatrix} 1 & 0 & 0 \\ 0 & 1 & 0 \\ 0 & 0 & -2 \end{bmatrix}$ and hence:

$$\ddot{\mathbf{s}} + 2[\boldsymbol{\omega}]\dot{\mathbf{s}} - \frac{1}{m_{CT}}\boldsymbol{\Lambda}\mathbf{s} = \frac{\mathbf{F}_{C_{th}}}{m_C} - \frac{\mathbf{F}_{T_{\epsilon\mu}}}{m_{CT}} + \Delta\mathbf{f}_p \tag{25}$$

with in the orbital frame:

$$\boldsymbol{\Lambda}_{\mathcal{O}} = m_{CT}\begin{bmatrix} \omega^2 - \frac{\mu}{r^3} & \eta_z & -\eta_y \\ -\eta_z & -\frac{\mu}{r^3} & \eta_x \\ \eta_y & -\eta_x & \omega^2 + \frac{2\mu}{r^3} \end{bmatrix} \tag{26}$$

$\boldsymbol{\Lambda}$ is hence a matrix depending only on the external parameters ω, η and r. Neglecting the differential accelerations on each spacecraft due to different perturbations yields finally:

$$\ddot{\mathbf{s}} + 2[\boldsymbol{\omega}]\dot{\mathbf{s}} - \frac{1}{m_{CT}}\boldsymbol{\Lambda}\mathbf{s} = \frac{\mathbf{F}_{C_{th}}}{m_C} - \frac{\mathbf{F}_{T_{\epsilon\mu}}}{m_{CT}} \tag{27}$$

If the orbit can be considered circular, $\boldsymbol{\eta}$ can be neglected. In this case, $\eta_{i,i\in\{x,y,z\}} = 0$ and $\omega^2 = \frac{\mu}{r^3}$. $\boldsymbol{\Lambda}$ can then be simplified in:

$$\boldsymbol{\Lambda}_{circ_{\mathcal{O}}} = m_{CT}\begin{bmatrix} 0 & 0 & 0 \\ 0 & -\omega^2 & 0 \\ 0 & 0 & 3\omega^2 \end{bmatrix} \tag{28}$$

4.3. Attitude dynamics including dipole lever-arm

In orbit, several perturbation torques apply to the satellites: the torque due to the gravity gradient, the torque due to the solar radiation, the torque due to the atmospheric drag, the torque due to the external magnetic field... In this study, we include the gravity gradient torque in the computation, which for satellite i is given by Curtis (2008):

$$\boldsymbol{\tau}_{i_g} = 3\frac{\mu}{r^3}\hat{\mathbf{z}}_{\mathcal{O}} \times \mathbf{J}_i\hat{\mathbf{z}}_{\mathcal{O}} \tag{29}$$

The torque due to the atmospheric drag and to the solar pressure are also taken into account, but included in the perturbation torque $\boldsymbol{\tau}_p$ which is assumed decorrelated from any other parameter. Their modeling would indeed be complex, and obtaining such an accuracy is not necessary.

The satellites considered are also subjected to magnetic torques in orbit: $\boldsymbol{\tau}_{i_{\epsilon\mu_E}}$ is the torque in satellite i due to the presence of the magnetic field of he Earth ($\boldsymbol{\tau}_{i_{\epsilon\mu_E}} = \boldsymbol{\mu}_i \times \mathbf{B}_E$). And $\boldsymbol{\tau}_{\epsilon\mu_{T/C}}$ for example is the torque on the chaser due to the presence of the magnetic field created by the target's dipole, and computed with (6):

$$\boldsymbol{\tau}_{\epsilon\mu_{T/C}} = \frac{\mu_0}{4\pi}\boldsymbol{\mu}_C \times \Gamma\boldsymbol{\mu}_T \tag{30}$$

Finally, $\boldsymbol{\tau}_{T_\gamma}$ is the torque created by the chaser on the target because of the lever-arm $\boldsymbol{\gamma}_{\mu_T}$ and the magnetic force $\mathbf{F}_{T_{\epsilon\mu}}$:

$$\boldsymbol{\tau}_{T_\gamma} = \boldsymbol{\gamma}_{\mu_T} \times \frac{3\mu_0}{4\pi}\boldsymbol{\Psi}_T\boldsymbol{\mu}_C \tag{31}$$

To these external torques is also added the torque created by the attitude control system of each satellite: $\boldsymbol{\tau}_{i_{rw}}$. For the target satellite $\boldsymbol{\tau}_{T_{rw}}$ can be set to 0 in a low cooperative scenario, or can be controlled in a fully-cooperative scenario (see Section 5.2).

In the body frame, the evolution of the attitude of one of the satellites is described by:

$$\mathbf{J}\frac{d\boldsymbol{\omega}_{T/\mathcal{I}}}{dt} + \boldsymbol{\omega}_{T/\mathcal{I}} \times \mathbf{J}\boldsymbol{\omega}_{T/\mathcal{I}} = \sum \boldsymbol{\tau} \tag{32}$$

For the target satellite, the attitude dynamics is hence governed by:

$$\mathbf{J}_T\frac{d\boldsymbol{\omega}_{T/\mathcal{I}}}{dt} + \boldsymbol{\omega}_{T/\mathcal{I}} \times \mathbf{J}_T\boldsymbol{\omega}_{T/\mathcal{I}} = \boldsymbol{\tau}_{T_{\epsilon\mu_C}} + \boldsymbol{\tau}_{T_\gamma} + \boldsymbol{\tau}_{T_{\epsilon\mu_E}} + \boldsymbol{\tau}_{T_g} + \boldsymbol{\tau}_{T_p} + \boldsymbol{\tau}_{T_{rw}} \tag{33}$$

The chaser satellite mass repartition is modeled by a homogeneous sphere. Therefore, no gravity gradient torques applies ($\boldsymbol{\tau}_{C_g} = \mathbf{0}$) and $\boldsymbol{\omega}_{\mathcal{C}/\mathcal{I}} \times \mathbf{J}_C\boldsymbol{\omega}_{\mathcal{C}/\mathcal{I}} = \mathbf{0}$. Its dipole is located at its center of mass, which nullifies the lever-arm torque: $\boldsymbol{\tau}_{C_\gamma} = \mathbf{0}$. The equation governing the chaser attitude is therefore:

$$\mathbf{J}_C\frac{d\boldsymbol{\omega}_{\mathcal{C}/\mathcal{I}}}{dt} = \boldsymbol{\tau}_{C_{\epsilon\mu_T}} + \boldsymbol{\tau}_{C_{\epsilon\mu_E}} + \boldsymbol{\tau}_{C_p} + \boldsymbol{\tau}_{C_{rw}} \tag{34}$$

The magnetic dipole of the chaser must be of order 10^6 Am^2 (see Section 7) for the application considered. In orbit at 700 km altitude, the value of the magnetic field of the Earth is of order 3×10^{-5} T. Hence, $\boldsymbol{\tau}_{C_{\epsilon\mu_E}}$ can reach values as high as 30 Nm. However, this perturbing torque can be counterbalanced by $\boldsymbol{\tau}_{C_{\epsilon\mu_T}}$.

The attitude of the chaser shall nominally remain equal to zero at all time: $\boldsymbol{\theta}_C = \mathbf{0}$. Then $\frac{d\boldsymbol{\omega}_{\mathcal{C}/\mathcal{I}}}{dt} = \frac{d\boldsymbol{\omega}_{\mathcal{O}/\mathcal{I}}}{dt} = \boldsymbol{\eta}$. Therefore, the value of $\mathbf{J}_C\boldsymbol{\eta}$ would typically be lower than 10^{-3} Nm, even for highly elliptical orbit as Geostationary Transfer Orbits. We include every torque neglected in our model in $\boldsymbol{\tau}_{C_p}$. As the sum $\mathbf{J}_C\boldsymbol{\eta} - \boldsymbol{\tau}_{C_p}$ is small, and as it is not fully modeled, it will be compensated by the Attitude Control System of the chaser:

$$\mathbf{J}_C\frac{d\boldsymbol{\omega}_{\mathcal{C}/\mathcal{I}}}{dt} = \boldsymbol{\tau}_{C_p} + \boldsymbol{\tau}_{C_{rw}} \tag{35}$$

This yields the necessary condition:

$$\mathbf{0} = \boldsymbol{\tau}_{C_{\epsilon\mu_E}} + \boldsymbol{\tau}_{C_{\epsilon\mu_T}} \tag{36}$$

4.3.1. Remark

One of the main contribution to the perturbation torque $\boldsymbol{\tau}_{C_p}$ is certainly the gyroscopic torque $\boldsymbol{\tau}_{C_h}$due to the angular

momentum $\mathbf{h}_{C_{rw}}$ stored in the chaser reaction wheel system. This torque reads $\boldsymbol{\tau}_{C_h} = -\boldsymbol{\omega}_{\mathcal{C}/\mathcal{I}} \times \mathbf{h}_{C_{rw}}$ and could be important with reaction wheels sized according to the high value of the chaser magnetic dipole. Nevertheless this torque in not taken into account in the design of the guidance law, which is the scope of this paper, but should be considered for the design of the control of the formation around the proposed guidance law.

4.4. Dynamics differential equations

In the sequel, the target attitude $\theta_{\mathbf{T}}$ is noted $\boldsymbol{\theta}$. We can now gather Eqs. (27), (33) and (36) into one differential system, which once solved will give the guidance of the formation:

$$\begin{cases} \ddot{\mathbf{s}} + 2[\boldsymbol{\omega}]\dot{\mathbf{s}} - \frac{1}{m_{CT}}\boldsymbol{\Lambda}\mathbf{s} = \frac{\mathbf{F}_{C_{th}}}{m_C} - \frac{\mathbf{F}_{T_{e\mu}}}{m_{CT}} \\ \mathbf{J}_T \frac{d\boldsymbol{\omega}_{T/\mathcal{I}}}{dt} + \boldsymbol{\omega}_{T/\mathcal{I}} \times \mathbf{J}_T \boldsymbol{\omega}_{T/\mathcal{I}} = \boldsymbol{\tau}_{T_{rw}} + \boldsymbol{\tau}_{T_{e\mu}} + \boldsymbol{\tau}_{T_\gamma} + \boldsymbol{\tau}_{T_{e\mu_E}} + \boldsymbol{\tau}_{T_g} + \boldsymbol{\tau}_{T_p} \\ \mathbf{0} = \boldsymbol{\tau}_{C_{e\mu_E}} + \boldsymbol{\tau}_{C_{e\mu_T}} \\ \boldsymbol{\omega}_{T/\mathcal{I}_T} = \mathbf{C}_2\dot{\boldsymbol{\theta}} - \omega \mathbf{P}_{\mathcal{O}\to\mathcal{T}}(\boldsymbol{\theta})[0 \quad 1 \quad 0]^T \end{cases} \tag{37}$$

which has been completed with the link between $\boldsymbol{\omega}_{T/\mathcal{I}_T}$ and $\boldsymbol{\theta}$, obtained from Wie (2008), with:

$$\mathbf{C}_2 = \begin{bmatrix} 1 & 0 & -\sin\theta_2 \\ 0 & \cos\theta_1 & \sin\theta_1\cos\theta_2 \\ 0 & -\sin\theta_1 & \cos\theta_1\cos\theta_2 \end{bmatrix} \tag{38}$$

5. Guidance strategies

5.1. Relative position strategy possibilities and consequences

At any time in orbit, forces have to be created on at least one of the satellites for the formation to be maintained, as it can be seen by nullifying the derivative terms in (27). These forces can either be created on the chaser only by its thruster, or on both satellites by the magnetic dipoles. In any case, the acceleration corresponding to these forces is given by (27) and is equal to $\left(\frac{1}{-m_{CT}}\boldsymbol{\Lambda}\mathbf{s}(2[\boldsymbol{\omega}]\dot{\mathbf{s}} + \ddot{\mathbf{s}})\right)$.

Words have been said about the orbit transfer thrust profile in Section 4.1. Let's write $\mathbf{F}_{C_{th_0}}$ this required thrust. For a given time t, a given transfer thrust $\mathbf{F}_{C_{th_0}}$ and a given relative position $\mathbf{s}, \mathbf{F}_{C_{th}}$ can be developed in the following way:

$$\mathbf{F}_{C_{th}} = \mathbf{F}_{C_{th_0}} - \alpha\frac{m_C}{m_{CT}}(\boldsymbol{\Lambda}\mathbf{s} - m_{CT}(2[\boldsymbol{\omega}]\dot{\mathbf{s}} + \ddot{\mathbf{s}})) \tag{39}$$

with $\alpha \in [01]$ a tuning parameter used to split the work required to maintain formation between the chaser thrust and the force created by the chaser's magnetic dipole, as explained in the following. Combining (39) with (27) leads to:

$$\mathbf{F}_{T_{e\mu}} = \frac{m_{CT}}{m_C}\mathbf{F}_{C_{th_0}} + (1-\alpha)(\boldsymbol{\Lambda}\mathbf{s} - m_{CT}(2[\boldsymbol{\omega}]\dot{\mathbf{s}} + \ddot{\mathbf{s}})) \tag{40}$$

which gives the magnetic force which has to be created by the chaser on the target, in order for the formation to follow the path given by $\mathbf{s}(t)$.

For a given time t (so a given matrix $\boldsymbol{\Lambda}$), a given transfer thrust $\mathbf{F}_{C_{th_0}}$ and a given relative position $\mathbf{s}$, several parameters α hence enable to maintain the formation together. The following sections will explain the impact of this parameter.

5.1.1. Minimum thrust strategy

One can, for example, choose $\alpha = 0$. In this case, the formation is maintained by the magnetic force only, as the thruster force is reduced to $\mathbf{F}_{C_{th_0}}$: no fuel is spent to maintain the formation together. In this case:

$$\mathbf{F}_{T_{e\mu}} = \frac{m_{CT}}{m_C}\mathbf{F}_{C_{th_0}} + \boldsymbol{\Lambda}\mathbf{s} - m_{CT}(2[\boldsymbol{\omega}]\dot{\mathbf{s}} + \ddot{\mathbf{s}}) \tag{41}$$

which corresponds to the acceleration imposed on both spacecraft. Then

$$\mathbf{F}_{C_{th}} = \mathbf{F}_{C_{th_0}} \tag{42}$$

So if $\mathbf{F}_{C_{th_0}} = \mathbf{0}$, then no thrust must be applied to the chaser. This corresponds to the strategy minimizing the thrust used.

5.1.2. Minimum dipole strategy

Another possibility is to choose $\alpha = 1$. Then the electromagnetic force created only serve as a propulsion for the target, and the formation is maintained due to the chaser thrust only. In this case:

$$\mathbf{F}_{T_{e\mu}} = \frac{m_{CT}}{m_C}\mathbf{F}_{C_{th_0}} \tag{43}$$

and

$$\mathbf{F}_{C_{th}} = \mathbf{F}_{C_{th_0}} - \frac{m_C}{m_{CT}}(\boldsymbol{\Lambda}\mathbf{s} - m_{CT}(2[\boldsymbol{\omega}]\dot{\mathbf{s}} + \ddot{\mathbf{s}})) \tag{44}$$

So if $\mathbf{F}_{C_{th_0}} = \mathbf{0}$, then no magnetic dipole needs to be created to maintain the formation in equilibrium. This effort would be supported by the thrust only.

5.1.3. Remarks

These two examples are underlined amongst the infinite number of possible values for α because the first one minimizes the fuel needed for the mission, and the second minimizes the magnetic dipole value. Indeed, for the first one, no thrust is needed to maintain the formation. Therefore the fuel is used only to modify the orbit of the target.

The second case minimizes the magnetic force which needs to be created on the target: its only effect is to act as thrust for the target. It does not help maintaining the formation. Hence, this scenario minimizes the chaser dipole module.

A representation of these two strategies can be found in Fig. 3, where the component of (39) are developed in the case of station keeping, without orbit transfer. Of course, α can be chosen arbitrarily. Choosing it between 0 and 1

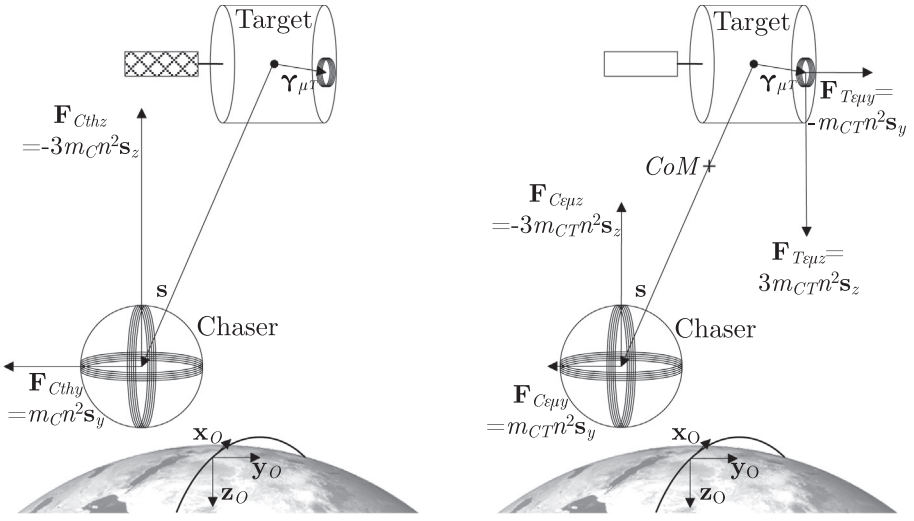

(a) Minimum dipole strategy ($\mathbf{F}_{C_{th_0}} = \mathbf{0}$, $\alpha = 1$, $\dot{\mathbf{s}} = \ddot{\mathbf{s}} = \mathbf{0}$)

(b) Minimum thrust strategy ($\mathbf{F}_{C_{th_0}} = \mathbf{0}$, $\alpha = 0$, $\dot{\mathbf{s}} = \ddot{\mathbf{s}} = \mathbf{0}$)

Fig. 3. Representation of the two strategies identified in Section 5. $\hat{\mathbf{x}}_{\mathcal{O}}$ is perpendicular to the drawing, $\hat{\mathbf{y}}_{\mathcal{O}}$ is toward the right, and $\hat{\mathbf{z}}_{\mathcal{O}}$ is directed to the bottom of the page. If $\mathbf{F}_{C_{th_0}} = \mathbf{0}$, the unique point which must be chosen to describe the orbit in the first case is the center of mass of the target. Indeed, the other points do not follow a Kelperian trajectory. In the second case, this point is the center of mass of the whole formation.

would have as effect to "share" the effort of formation keeping between the two forces.

5.2. Attitude dynamics strategy possibilities and consequences

Two magnets interacting create at the same time forces and torques on each other, unless they are in very particular configurations. Therefore, it is not possible to choose the attitude of both satellites without creating strong magnetic torques on both of them. Indeed, although these torques could be counterbalanced by the attitude control system of both satellites for a short time, these attitude control systems would quickly saturate.

However, even if choosing the target satellite's attitude is not possible, its attitude control system can be used to slightly modulate its behavior. To do so, a tuning parameter β is introduced, which modifies the torque created by the target's attitude control system. The aim is to modify the solutions found in Section 6, by creating a torque conveniently chosen:

$$\boldsymbol{\tau}_{T_{rw}} = \beta\left(\mathbf{J}_T\frac{d\boldsymbol{\omega}_{T/\mathcal{I}}}{dt} + \boldsymbol{\omega}_{T/\mathcal{I}}\times\mathbf{J}_T\boldsymbol{\omega}_{T/\mathcal{I}}\right) \tag{45}$$

with $\beta \in \mathbb{R}$. (33) then reads:

$$(1-\beta)\left(\mathbf{J}_T\frac{d\boldsymbol{\omega}_{T/\mathcal{I}}}{dt} + \boldsymbol{\omega}_{T/\mathcal{I}}\times\mathbf{J}_T\boldsymbol{\omega}_{T/\mathcal{I}}\right) = \boldsymbol{\tau}_{T_{\epsilon\mu}} + \boldsymbol{\tau}_{T_\gamma} + \boldsymbol{\tau}_{T_{\epsilon\mu_E}} + \boldsymbol{\tau}_{T_g} + \boldsymbol{\tau}_{T_p} \tag{46}$$

5.2.1. Fully-cooperative configuration

In some scenarios, it might be very well possible to provide a required attitude to the target, as well as a nominal torque to apply. In these cases, the attitude control system of the target could satisfy $\beta = 1$. Then (46) becomes:

$$\mathbf{0} = \boldsymbol{\tau}_{T_{\epsilon\mu}} + \boldsymbol{\tau}_{T_\gamma} + \boldsymbol{\tau}_{T_{\epsilon\mu_E}} + \boldsymbol{\tau}_{T_g} + \boldsymbol{\tau}_{T_p} \tag{47}$$

5.2.2. Low-cooperative configuration

In some other scenarios, it might be impossible for the chaser to establish a communication with the target. In this case, the target satellite is supposed ro be passive, but not hostile to the tugging. Then it is safe to assume $\beta = 0$, and (46) becomes:

$$\mathbf{J}_T\frac{d\boldsymbol{\omega}_{T/\mathcal{I}}}{dt} + \boldsymbol{\omega}_{T/\mathcal{I}}\times\mathbf{J}_T\boldsymbol{\omega}_{T/\mathcal{I}} = \boldsymbol{\tau}_{T_{\epsilon\mu}} + \boldsymbol{\tau}_{T_\gamma} + \boldsymbol{\tau}_{T_{\epsilon\mu_E}} + \boldsymbol{\tau}_{T_g} + \boldsymbol{\tau}_{T_p} \tag{48}$$

5.3. Summarizing guidance differential equations

This last development lets us update (37) in:

$$\begin{cases} \mathbf{0} = \frac{m_{CT}}{m_C}\mathbf{F}_{C_{th_0}} - \mathbf{F}_{T_{\epsilon\mu}} + (1-\alpha)(\boldsymbol{\Lambda}\mathbf{s} - m_{CT}(2[\boldsymbol{\omega}]\dot{\mathbf{s}} + \ddot{\mathbf{s}})) \\ \mathbf{0} = \boldsymbol{\tau}_{T_{\epsilon\mu}} + \boldsymbol{\tau}_{T_\gamma} + \boldsymbol{\tau}_{T_{\epsilon\mu_E}} + \boldsymbol{\tau}_{T_g} + \boldsymbol{\tau}_{T_p} \\ \qquad -(1-\beta)\left(\mathbf{J}_T\frac{d\boldsymbol{\omega}_{T/\mathcal{I}}}{dt} + \boldsymbol{\omega}_{T/\mathcal{I}}\times\mathbf{J}_T\boldsymbol{\omega}_{T/\mathcal{I}}\right) \\ \mathbf{0} = \boldsymbol{\tau}_{C_{\epsilon\mu_E}} + \boldsymbol{\tau}_{C_{\epsilon\mu_T}} \\ \mathbf{0} = \boldsymbol{\omega}_{T/\mathcal{I}_T} - \mathbf{C}_2\dot{\boldsymbol{\theta}} + \omega\mathbf{P}_{\mathcal{O}\to\mathcal{T}}[0 \quad 1 \quad 0]^T \end{cases} \tag{49}$$

6. Guidance problem resolution

Relative configuration guidance for EMFF during orbit transfer does not seem solved in the litterature. Some

authors showed solutions for very particular cases (Zhang et al., 2014), but even in these cases, the attitude dynamics of the satellites were not taken into account. Moreover, earlier studies considered EMFF satellites as being orbiting magnets, and the location of magnetic dipole inside satellites was tacitly supposed perfectly centered.

For EMFF in general, requirements on the torques are often neglected: to our knowledge, only Schweighart (2005) tried to minimize them. However, creating forces between two magnets also creates a torque on both, even without taking into account the Earth magnetic field, which can create torques of order reaching 30 Nm for dipoles of order 10^6 Am^2 in low Earth orbit. In general, this problem is left to the control. Indeed, the suggestion widely spread in the literature is to wave the dipoles of all satellites in the formation, in order to average the magnetic torque to zero, in order to keep the angular momentum stored in the reaction wheels at relatively low values (Ahsun et al., 2007; Hashimoto et al., 2002).

In this study, this problem is solved differently: while in general the relative position of the satellites in the formation is given and the torques are not chosen, the torques are here compensated but the relative position is free.

6.1. Combining dynamics and magnetics

Section 3 has fixed a way of writing magnetic forces and torques. Sections 4 and 5 lead to the model (49), which needs to be solved to get the solution of the guidance transfer. Let's now combine these results. Doing so leads to the following system:

$$\begin{cases} \mathbf{0} = \frac{m_{CT}}{m_C}\mathbf{F}_{C_{ith_0}} - \frac{3\mu_0}{4\pi}\boldsymbol{\Psi}_T\left(\boldsymbol{\mu}_T, \boldsymbol{\gamma}_{\mu_T} - \mathbf{s}\right)\boldsymbol{\mu}_C \\ \quad +(1-\alpha)(\boldsymbol{\Lambda}\mathbf{s} - m_{CT}(2[\boldsymbol{\omega}]\dot{\mathbf{s}} + \ddot{\mathbf{s}})) \\ \mathbf{0} = \boldsymbol{\mu}_T \times \left(\frac{\mu_0}{4\pi}\Gamma\left(\boldsymbol{\gamma}_{\mu_T} - \mathbf{s}\right)\boldsymbol{\mu}_C + \mathbf{B}_E\right) \\ \quad +\boldsymbol{\gamma}_{\mu_T} \times \frac{3\mu_0}{4\pi}\boldsymbol{\Psi}_T\left(\boldsymbol{\mu}_T, \boldsymbol{\gamma}_{\mu_T} - \mathbf{s}\right)\boldsymbol{\mu}_C \\ \quad +\boldsymbol{\tau}_{T_g}(\boldsymbol{\theta}) + \boldsymbol{\tau}_{T_p} - (1-\beta)\left(\mathbf{J}_T\frac{d\boldsymbol{\omega}_{T/\mathcal{I}}}{dt} + \boldsymbol{\omega}_{T/\mathcal{I}} \times \mathbf{J}_T\boldsymbol{\omega}_{T/\mathcal{I}}\right) \\ \mathbf{0} = \boldsymbol{\mu}_C \times \left(\frac{\mu_0}{4\pi}\Gamma\left(\boldsymbol{\gamma}_{\mu_T} - \mathbf{s}\right)\boldsymbol{\mu}_T + \mathbf{B}_E\right) \\ \mathbf{0} = \boldsymbol{\omega}_{T/\mathcal{I}_T} - \mathbf{C}_2\dot{\boldsymbol{\theta}} + \omega\mathbf{P}_{\mathcal{O}\to\mathcal{T}}(\boldsymbol{\theta})\begin{bmatrix}0 & 1 & 0\end{bmatrix}^T \end{cases} \tag{50}$$

The unknowns are: $\mathbf{s}_{\mathcal{O}} = \begin{bmatrix} s_{x_{\mathcal{O}}} & s_{y_{\mathcal{O}}} & s_{z_{\mathcal{O}}} \end{bmatrix}^T$, representing the relative position of the chaser spacecraft's center of mass with respect to the target spacecraft's center of mass in the orbital frame; $\boldsymbol{\omega}_{T/\mathcal{I}_T} = \begin{bmatrix} p_T & q_T & r_T \end{bmatrix}^T$, representing the inertial angular rate of the target spacecraft in its body frame; $\boldsymbol{\theta} = \begin{bmatrix} \theta_1 & \theta_2 & \theta_3 \end{bmatrix}^T$, representing the Euler angles describing the attitude of the target spacecraft with regard to the orbital frame; $\boldsymbol{\mu}_{C_{\mathcal{O}}} = \begin{bmatrix} \mu_{C_{x_{\mathcal{O}}}} & \mu_{C_{y_{\mathcal{O}}}} & \mu_{C_{z_{\mathcal{O}}}} \end{bmatrix}^T$, representing the chaser magnetic dipole in orbital frame.

The knowns are the physical parameters describing the formation: the dipole of the target $\boldsymbol{\mu}_T$, its lever-arm $\boldsymbol{\gamma}_{\mu_T}$, the formation reduced mass m_{CT}, the target inertia matrix $\mathbf{J}_T$; the parameters depending on the orbit: the rotation vector from inertial to orbital frame $\boldsymbol{\omega}$, its time derivative $\boldsymbol{\eta}$, the Earth magnetic field $\mathbf{B}_E$; the strategy parameters: α, β and the given transfer thrust $\mathbf{F}_{C_{ith_0}}$.

6.2. Solving the equations: continuation principle

Solving the guidance problem is not straight forward. Indeed, it is constituted of 12 equations, has 12 unknowns, and is not linear. Even if the time derivative were set to zero, developing $\Gamma\left(\boldsymbol{\gamma}_{\mu_T} - \mathbf{s}\right)$ and $\boldsymbol{\Psi}_T\left(\boldsymbol{\mu}_T, \boldsymbol{\gamma}_{\mu_T} - \mathbf{s}\right)$ and substituting their expressions in (50) reveals a polynomial system in $s_x, s_y, s_z, \mu_{C_x}, \mu_{C_y}, \mu_{C_z}$, and sine and cosine of $\theta_1, \theta_2, \theta_3$. The non linearity of this kind of equations makes the existence and number of solutions unsure, even in the static case. (Consider for example the three systems

$$\begin{cases} x^2 + y^2 - k = 0 \\ x^4 - y^4 - 2x^2 + 1 = 0 \end{cases}, \quad k \in \left\{\frac{1}{2}, 1, 2\right\} \tag{51}$$

which have respectively zero, an infinite number of solutions and four solutions.)

A system having a finite number of solutions is easier to handle than a system having an infinite number of solutions. Indeed, in the first case, initializing carefully a gradient-based method enables to find several solutions, if not all of them. To transform a system in order to have a finite number of solutions, one can choose one of the variables as a parameter, and then solve the system.

To find every solution of the problem numerically, a continuation method can be used. The principle is to choose a variable as a parameter and to make it evolve slowly, in order for the solutions to evolve slowly as well. Initializing a new numerical resolution with the result given by the previous one then enables to follow the evolution of the solutions. This principle is illustrated in Fig. 4 for (51) with $k = 1$. It enables to get a set of solutions which are representative of the infinite number of solutions. It can be noted here that the continuation method used is different from the one used in Schweighart (2005). Indeed while Schweighart used a continuation method on the *equations* themselves (i.e. starting with simple polynomial equations, and making them more complex at each step), we are using a continuation method on the *solutions*. This is justified by two facts: (i) contrary to Schweighart who wanted to find every possible solutions to the problem, we are looking only for one viable solution; (ii) the continuation method is also used to find the evolution of the guidance solution in time, as it will be seen in Section 6.4.

6.3. Solving the equations: initial configuration solutions

(50) is a differential system. Its resolution will be completely showed in Section 6.4. However, as any differential equation, the solution found depends on the initial condi-

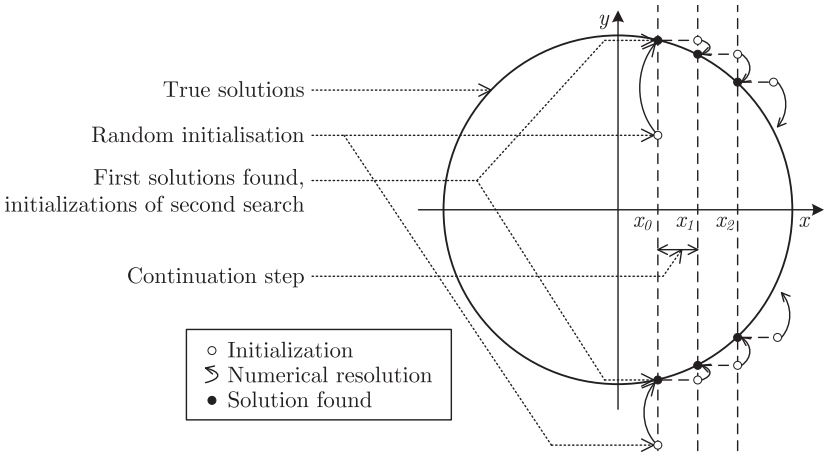

Fig. 4. Continuation method principle.

tion. This initial condition represents in our case the beginning of the interaction between the chaser and the target. Finding a good configuration for this beginning is not trivial, but falls directly under what has been developed previously. It is imposed that at the beginning, the satellites in the formation are not moving relatively to one another, and have no attitude motion. The equation to solve (in $\mathbf{s}, \boldsymbol{\mu}_C, \boldsymbol{\theta}$ and $\boldsymbol{\omega}_{\mathcal{T}/\mathcal{I}}$) is therefore the system (50), in which the time derivative terms are set to zero. Hence:

$$\begin{cases} \mathbf{0} = \frac{m_{CT}}{m_C}\mathbf{F}_{C_{th_0}} - \frac{3\mu_0}{4\pi}\boldsymbol{\Psi}_T\left(\boldsymbol{\mu}_T, \gamma_{\mu_T} - \mathbf{s}\right)\boldsymbol{\mu}_C + (1-\alpha)\boldsymbol{\Lambda}\mathbf{s} \\ \mathbf{0} = \boldsymbol{\mu}_T \times \left(\frac{\mu_0}{4\pi}\Gamma\left(\gamma_{\mu_T} - \mathbf{s}\right)\boldsymbol{\mu}_C + \mathbf{B}_E\right) \\ \quad + \boldsymbol{\gamma}_{\mu_T} \times \frac{3\mu_0}{4\pi}\boldsymbol{\Psi}_T\left(\boldsymbol{\mu}_T, \gamma_{\mu_T} - \mathbf{s}\right)\boldsymbol{\mu}_C \\ \quad + \boldsymbol{\tau}_{T_g}(\boldsymbol{\theta}) + \boldsymbol{\tau}_{T_p} - (1-\beta)(\mathbf{J}_T\boldsymbol{\eta} + \boldsymbol{\omega} \times \mathbf{J}_T\boldsymbol{\omega}) \\ \mathbf{0} = \boldsymbol{\mu}_C \times \left(\frac{\mu_0}{4\pi}\Gamma\left(\gamma_{\mu_T} - \mathbf{s}\right)\boldsymbol{\mu}_T + \mathbf{B}_E\right) \\ \boldsymbol{\omega}_{\mathcal{T}/\mathcal{I}} = s\boldsymbol{\omega} \end{cases} \tag{52}$$

which is a quasi-polynomial system, for which we apply the method described in Section 6.2. An example of possible solutions is given in Fig. 5: it represents the set of initial positions $\mathbf{s}$ which can be chosen for the chaser, relatively

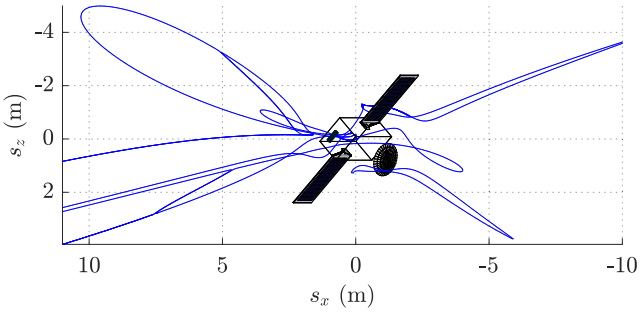

Fig. 5. Example of relative position solutions to the static guidance problem in the scenario II (see Table 2) with $\alpha = \beta = 0$. $s_y \simeq 0$ for every point. Lines indicate admissible initial chaser location. Target is represented at the center of the frame in attitude corresponding to one solution. Frame is orbital: Earth at the bottom, orbital velocity toward left.

to the target located at the center of the frame. This set of solutions can be reduced to take into account a minimal chaser-target distance to avoid collisions (see next section). To any of the position solutions is associated a chaser magnetic dipole $\boldsymbol{\mu}_C$ and an orientation $\boldsymbol{\theta}$ of the target, which are not represented. The chaser's attitude is always equal to zero in the orbital frame. The frame is the orbital frame centered on the target. The values chosen for the different parameters are given in Table 1.

6.4. Solving the differential system: forward euler scheme

The previous section has dealt with the initialisation of the differential equation resolution. The resolution through time is detailed here.

Because of the complexity of the differential system, looking for analytical solutions does not seem realistic. Indeed, the system is not only non-linear, but it is time-varying: as mentioned earlier, $\mathbf{F}_{C_{th_0}}$ could be varied through the orbit. Moreover, the parameters $r, \boldsymbol{\omega}$ and $\boldsymbol{\eta}$ are not constant if the orbit is not circular, and $\mathbf{B}_{E_\mathcal{O}}$ is not constant in any case.

The differential system is therefore solved numerically, with a time step of 5 s. To do so, the time derivatives of the unknowns are computed in a forward Euler scheme: at time-step n, the time derivatives are computed as polynomials of the previous and current unknowns. Here is given the example for $\mathbf{s}$:

$$\begin{aligned} \dot{\mathbf{s}}_n &= \frac{\mathbf{s}_n - \mathbf{s}_{n-1}}{dt} \\ \ddot{\mathbf{s}}_n &= \frac{\mathbf{s}_n - 2\mathbf{s}_{n-1} + \mathbf{s}_{n-2}}{dt^2} \end{aligned} \tag{53}$$

Combining this with system (50) then yields a system close to (52). Its resolution is therefore treated the same way. This however, is not enough to completely solve the guidance problem, as solving this new system gives an infinite number of solutions. To choose amongst them, a cost function is designed, which goal is to keep the distance between both satellites roughly constant. The solution minimizing

Table 1
Parameters and initial configuration used in the case study.

Mass of target (m_T)	2300 kg
Target inertia matrix ($\mathbf{J}_{T_T}$)	diag([1300 1100 700]) kg·m^2
Mass of chaser (m_C)	1000 kg
Chaser inertia matrix ($\mathbf{J}_{C_c}$)	diag([700 700 700]) kg·m^2
Target dipole ($\boldsymbol{\mu}_{T_T}$)	$[0\,5000]^T$ Am^2
Target dipole position in body frame ($\boldsymbol{\gamma}_{\mu_{T_T}}$)	$[1\,0\,0]^T$ m
Maximum chaser dipole value ($\|\boldsymbol{\mu}_C\|$)	10^7 Am^2
Nominal transfer thrust ($\mathbf{F}_{C_{th_{0_\mathcal{O}}}}$)	$[5000]^T$ mN
Target disturbing torque ($\boldsymbol{\tau}_{C_p}$)	$[0\,0\,0]^T$ Nm
Initial configuration:	$\boldsymbol{\theta}_C = 0; \dot{\boldsymbol{\theta}}_C = 0; \dot{\boldsymbol{\theta}} = 0; \dot{\mathbf{s}} = 0$ ($\boldsymbol{\theta}$ and $\mathbf{s}$ solution of Eq. (52))
Initial true anomaly	0

the cost function is selected amongst the solutions of the system:

$$cost(\mathbf{s}) = (\|\mathbf{s}\| - s_{desired})^2 \tag{54}$$

where $s_{desired}$ is the desired distance between the two satellites. $s_{desired}$ is chosen so that at the beginning of the interaction, $\|\boldsymbol{\mu}_C\| = 10^6$ Am^2.

7. Results

Testing has been realized in a wide range of orbits with the parametric configuration in Table 1. In this section, two particular scenarios, defined in Table 2, are presented and analyzed: circular equatorial orbits, because of its periodicity, and circular Sun-synchronous orbits. The latter are studied for two reasons. First, because they represent a major difficulty caused by the quickly varying Earth magnetic field at the poles. Second, because this kind of orbit is particularly used by Earth observation satellites, which represent potential targets in the frame of ADR.

7.1. Equatorial orbits

Circular equatorial orbits (scenario I) are the only one for which the parameters $r, \boldsymbol{\omega}, \boldsymbol{\eta}$ and above all $\mathbf{B}_{E_\mathcal{O}}$ are trivially time-periodic. Let us therefore pay attention to this situation.

As one can see from (49), if α and β are set to 1, then the model becomes a set of time dependent algebraic equations. The periodicity of the constants will make the guidance solution periodic also. This can be seen in Fig. 6, from the fact that the trajectory of the chaser relatively to the target along the orbit is closed. Fig. 7 presents the evolution of the Earth magnetic field in orbital frame during 2 orbits, as well as the evolution of all the states. From top to bottom, each plot presents the three axis orbital-frame components of: surrounding magnetic field; relative position; target attitude; chaser magnetic dipole; chaser thruster force.

Table 2
Case study.

	Scenario I	Scenario II
Orbit	Circular equatorial	Circular sun-synchronous
Inclination	0 deg	98.2 deg
Altitude	805 km	705 km
RAAN	–	45 deg

RAAN: Right Ascension of the Ascending Node.

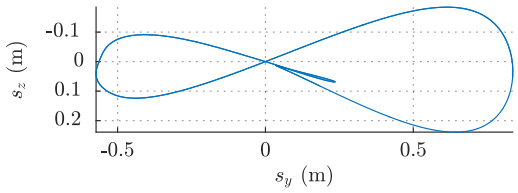

Fig. 6. Trajectory of the chaser relatively to the target in the orbital frame centered on the target in the scenario I with $\alpha = \beta = 1, s_{desired} = 9.1$ m. It corresponds to the trajectory of the chaser as seen from the target location, looking in the direction of the velocity vector. Setting $\alpha = \beta = 1$ makes (49) static, thus the periodicity of the external conditions make the solution periodic.

7.2. Sun-synchronous orbits: minimum thrust and low-cooperative target

Sun-synchronous orbits are orbits used by many Earth-observation satellites, because they have the particularity of keeping the lighting of the observed area constant at every passage of the satellite observing. They are orbits which have been identified for ADR, because of their high satellite density (Voirin et al., 2012). In this context, let us analyze the possibility to tug a satellite on which only the MTQ is still functioning. This represents low-cooperative cases, which could typically exist when de-orbiting a satellite having emptied its fuel tank and lost its AOCS. In this case the target could not ensure its own attitude stability, hence $\beta = 0$. As the aim would be to spare the fuel of the chaser, one could choose $\alpha = 0$. The result of the guidance in such a case is given in Figs. 8 and 9.

7.3. Sun-synchronous orbits: minimum dipole and low-cooperative target

As one can see on the 3D representation of the relative position evolution through two orbits, choosing $\alpha = \beta = 0$ makes the relative movement of the chaser around the target quite large. If one prefers (for safety reasons for example) to restrict the movement to a smaller volume, one can choose to increase α. Imposing $\alpha = 1$ corresponds to the case where the magnetic force is created only to provide the acceleration needed for the orbit transfer to the target. The results of the guidance in this case is given in Figs. 10 and 11. As it can be seen in Fig. 10, the force $\mathbf{F}_{C_{th}}$ created by the chaser differs from $\mathbf{F}_{C_{th_{0_\mathcal{O}}}} = [5000]^T$ mN. It is not a problem for the mission however: as explained in Section 5.1.2, the magnetic force created on the target is at all time equal to $\frac{m_{CT}}{m_C}\mathbf{F}_{C_{th_0}}$, ensuring that it follows the orbit

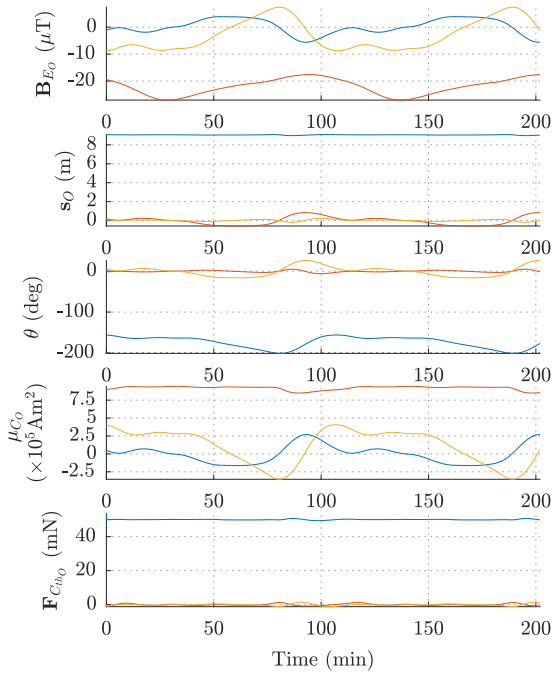

Fig. 7. Guidance path in the scenario I with $\alpha = \beta = 1, s_{desired} = 9.1$ m. The period of all parameters is equal to the synodic period of the movement, which takes into account the rotation of the Earth and is therefore different from the orbital period. Blue, red and yellow lines represent respectively x, y, and z axis for vectors and Euler angle 1, 2 and 3 for attitudes. First graph represents the Earth's magnetic field in frame $\mathcal{O}$. Second graph represents relative position $\mathbf{s}$ in frame $\mathcal{O}$. Third graph represents target attitude $\boldsymbol{\theta}$. Fourth graph represents chaser dipole $\boldsymbol{\mu}_C$ in frame $\mathcal{O}$. Fifth graph represents chaser thrust $\mathbf{F}_{C_{th}}$ in frame $\mathcal{O}$. (For interpretation of the references to color in this figure legend, the reader is referred to the web version of this article.)

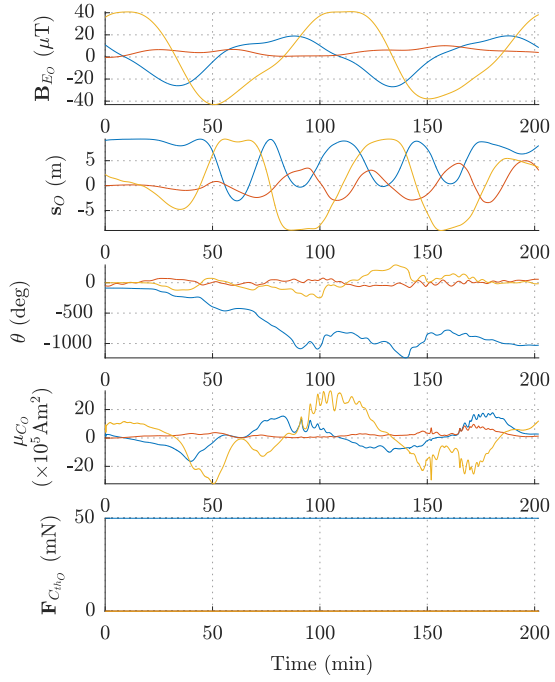

Fig. 8. Guidance path in the study case I with $\alpha = \beta = 0, s_{desired} = 9.3$ m. Legend details given in Fig. 7.

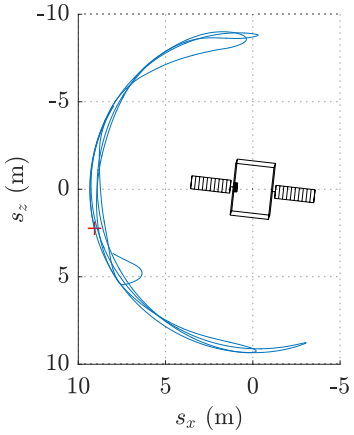

Fig. 9. Relative trajectory in the scenario II with $\alpha = \beta = 0, s_{desired} = 9.3$ m. View from the side: orbital velocity toward left, Earth toward bottom. Choosing $\alpha = \beta = 0$ makes the relative movement very large.

designed for the transfer. The only drawback is the increased fuel consumption by the chaser.

7.4. Angular momentum management

In the Section 4.3, care has been taken in order to avoid building angular momentum in both satellites during the orbit transfer: the Earth magnetic torque on the chaser has been balanced in (36); and the target AOCS torque has been taken into account in (33) where it can be set to zero. However, to control their attitude around the nomi-

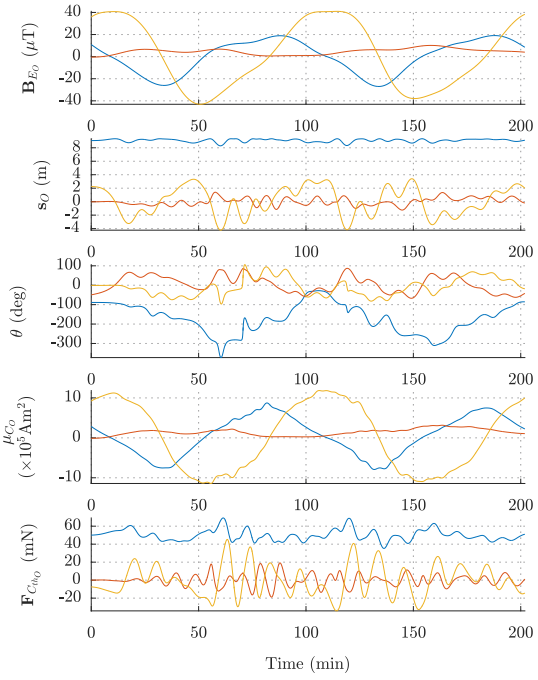

Fig. 10. Guidance path in the scenario II with $\alpha = 1, \beta = 0$ and $s_{desired} = 9.3$ m. As the attitude of the target is not controlled by its AOCS ($\beta = 0$), it oscillates around what could be a smooth evolution, causing the other parameters to do the same. Legend details given in Fig. 7.

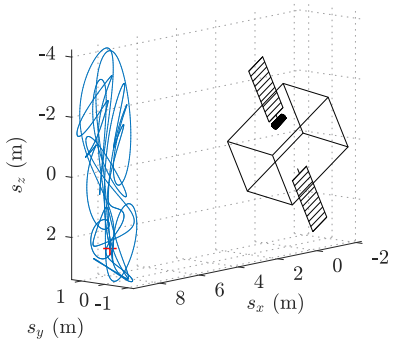

Fig. 11. Relative trajectory in the scenario II with $\alpha = 1, \beta = 0$ and $s_{desired} = 9.3$ m. The oscillations due to $\beta = 0$ are visible, but compared to Fig. 9, imposing $\alpha = 1$ has been efficient to constraint the relative movement to a smaller volume. Frame is orbital.

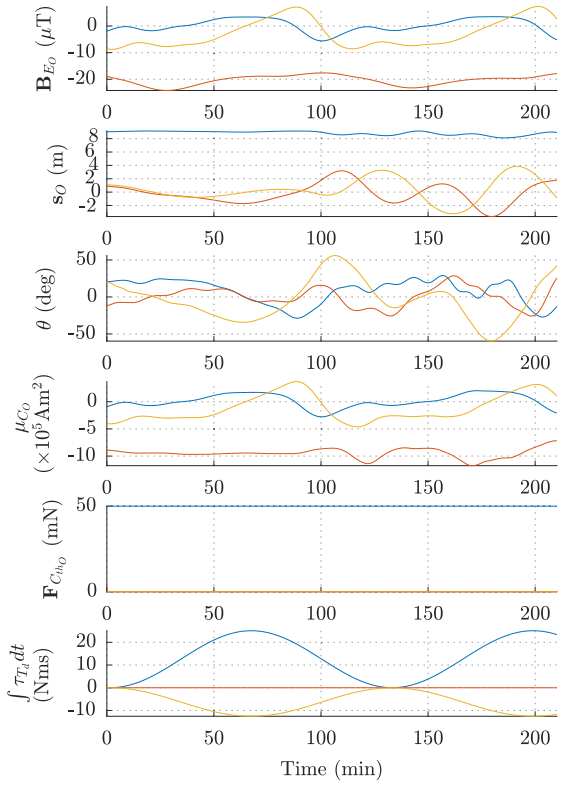

Fig. 12. Guidance path in the scenario I with $\alpha = \beta = 0$ and $s_{desired} = 9.1$ m. The last plot represents the angular momentum variation in the AOCS of the target, which is modulated without affecting the mission. Legend details given in Fig. 7.

nal value given by the guidance, chaser and target (in the cooperative scenario) might use reaction wheels or control momentum gyroscopes, as these devices have the advantage of not needing fuel. The drawback however is the limit of angular momentum they can store, which is driven by the maximal angular velocity withstood by their different rotating parts.

To desaturate reaction wheels, an external torque has to be created, so that opposing it decreases the angular momentum stored. In the chaser case, this torque can be

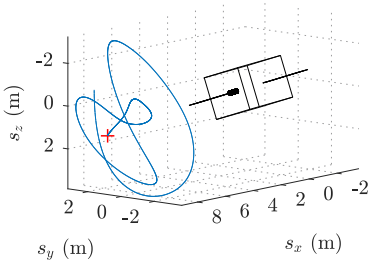

Fig. 13. Relative trajectory in the scenario I with $\alpha = \beta = 0$ and $s_{desired} = 9.1$ m during reaction wheels desaturation. Frame is orbital.

easily created thanks to the thrusters, which are continuously thrusting to modify the orbit. The orientation of the chaser is not fixed by the guidance. Therefore, one can choose its orientation in order to create the desired torque, depending on the location of the thruster on the chaser.

The target however does not have the capacity of creating a torque using thrusters. But one can take this need into account in (33), which then becomes:

$$\mathbf{J}_T \frac{d\boldsymbol{\omega}_{T/\mathcal{I}}}{dt} + \boldsymbol{\omega}_{T/\mathcal{I}} \times \mathbf{J}_T \boldsymbol{\omega}_{T/\mathcal{I}} = \boldsymbol{\tau}_{T_{\epsilon\mu_C}} + \boldsymbol{\tau}_{T_\gamma} + \boldsymbol{\tau}_{T_{\epsilon\mu_E}} + \boldsymbol{\tau}_{T_g} + \boldsymbol{\tau}_{T_p} + \boldsymbol{\tau}_{T_d} \quad (55)$$

where $\boldsymbol{\tau}_{T_d}$ is the torque which must be created by the reaction wheels to desaturate themselves. This torque does not have to be constant in time. In Figs. 12 and 13, an example is given where $\boldsymbol{\tau}_{T_d}$ is sinusoidal. The evolution of the target angular momentum is plotted in the last graph of Fig. 12. In this example, the maximum desaturation rate considered is 0.67 Nms/min, which seems enough to desaturate the target AOCS. More details can be obtained on the AOCS de-saturation in Fabacher (2016).

8. Conclusion

In some cases, it might be interesting to use a chaser satellite to magnetically tug a target satellite to another orbit. Doing so is not straight forward. Indeed, creating magnetic forces between two satellites immediately creates torques on both satellites, not only caused by the other satellite, but also because of the presence of the Earth's magnetic field. The existence of configuration paths satisfying the dynamics of the formation as well as the propulsion requirement is therefore not trivial, even without taking into account the time varying nature of several parameters of the problem.

This paper has hence reached several goals. First, it has developed a new framework to describe magnetic forces and torques in the far field domain, which enables to simply write them as matrices, making it easy to use. This paper above all demonstrated that magnetic tugging of target satellites is theoretically possible, even if the formation is not fully cooperative and the target is under-actuated. It also gave a way to obtain the solution of the guidance

problem for this orbit transfer, satisfying the dynamics of the formation, not only for the relative position, but also for the attitude of both satellites. This solution has been given taking into account the lever arm between the target center of mass and the position of its dipole, therefore demonstrating that every satellites using magnetorquers can be potential targets for the orbit transfer. Finally, a solution alternative to the dipole polarity switching has been proposed to avoid the building of angular momentum caused by the Earth magnetic field on both satellites for this particular application.

The control of the formation around the nominal guidance path found in this article has not been discussed, but the reader can find some initial work on this subject in Fabacher et al. (2016). In addition, the stability of the formation around the guidance path defined is discussed in Fabacher (2016). In this reference, non-linear simulations are used to ensure it. Further works are still to be performed to evaluate the robustness of the overall approach in spite of navigation errors, Earth magnetic field model errors, sensors and actuators imperfections. Finally, in the frame of this early-phase feasibility study, the modification of the dynamics due to the angular momentum stored by both satellites in their AOCS has not been taken into account. This shall be performed in future work.

Acknowledgement

E. Fabacher wishes to thank the European Space Agency and Airbus-Safran Launchers for funding his Ph. D. in the frame of ESA Network Partnership Initiative.

References

Ahsun, U., 2007. Dynamics and control of electromagnetic satellite formations. Ph.D. thesis, Massachusetts Institute of Technology.

Ahsun, U., Miller, D.W., Ramirez-Riberos, J.L., 2010. Control of electromagnetic satellite formations in near-earth orbits. J. Guid. Control Dynam.

Coverstone-Carroll, V., Hartmann, J.W., Mason, W.J., 2000. Optimal multi-objective low-thrust spacecraft trajectories. Comput. Methods Appl. Mech. Eng. 186, 387–402.

Curtis, D., 2008. Orbital mechanics for engineering students. In: Elsevier Aerospace Engineering Series. Elsevier.

Elias, L.M., Kwon, D.W., Sedwick, R.J., Miller, D.W., 2007. Electromagnetic formation fight dynamics including reaction wheel gyroscopic stiffening effects. J. Guid. Control Dynam.

Fabacher, E., Lizy-Destrez, S., Alazard, D., Ankersen, F., Jourdas, J.-F., 2015. Guidance and Navigation for Electromagnetic Formation Flight Orbit Modification. EuroGNC, Toulouse

Fabacher, E., Alazard, D., Ankersen, F., Lizy-Destrez, S., de Mijolla, L., 2016. Control for Magnetic Space Tug. In: IFAC Symposium on Automatic Control in Aerospace. Sherbrooke

Fabacher, E., 2016. Guidance and Control for Magnetic Space Tug. PhD thesis, ISAE-SUPAERO

Garrett, H.B., 1981. The charging of spacecraft surface. Rev. Geophys.

Hashimoto, T., Sakai, S-I., Ninomiya, K., Maeda, K., Saitoh, T., 2002. Formation Flight Control Using Super-Conducting Magnets Toulouse. France

Huang, X., Zhang, C., Ban, X., 2016. Dipole solution and angular-momentum minimization for two-satellite electromagnetic formation flight. Acta Astronaut.

Pergola, P., 2010. Low-thrust transfer to Backflip orbits. Adv. Space Res. 46, 1280–1291.

Petropoulos, A.E., 2002. Some analytic integrals of the averaged variational equations for a thrusting spacecraft. Interplanet. Netw. Prog. Rep. 150, 1–29.

Schaub, H., Sternovsky, Z., 2014. Active space debris charging for contactless electrostatic disposal maneuvers. Adv. Space Res.

Sakai, S., Kaneda, R., Maeda, K., Saitoh, T., Saito, H., Hashimoto, T., 2008. Electromagnetic formation flight for LEO satellites. In: 17th Workshop on JAXA Astrodynamics and Flight Mechanics.

Schweighart, S.A., 2005. Electromagnetic formation flight dipole solution planning. Ph.D. thesis, Massachusetts Institute of Technology.

Tsien, H.S., 1953. Take-off from satellite orbit. J. Am. Rocket Soc. 23 (4), 233–236.

Villani, D.D., 1998. An analytic solution for the force between two magnetic dipoles. Magnetic Electr. Separation 9, 39–52.

Voirin, T., Kowaltschek, S., Dubois-Matra, O., 2012. *NOMAD*: a contactless technique for active large debris removal. IAC-12.

Wie, B., 2008. Space Vehicle Dynamics and Control, Second ed. AIAA Education Series. American Institute of Aeronautics and Astronautics.

Zhang, Y.-w., Yang, L.-p., Zhu, Y.-w., Huang, H., 2014. Dynamics and solutions for multispacecraft electromagnetic orbit correction. J. Guid. Control Dynam. 37 (5), 1604–1610.